J Math Chem (2014) 52:2183–2196
DOI 10.1007/s10910-014-0374-5

ORIGINAL PAPER

Chaos in oscillatory sorption of hydrogen in palladium

Erwin Lalik

Received: 19 May 2014 / Accepted: 10 June 2014 / Published online: 28 June 2014

Abstract Aperiodic oscillations in the sorption of hydrogen and deuterium in palladium have been observed. An expression relating the square of a function, with the derivative and integral with variable upper limit of the same function has been proved and proposed to be used as a base for a chaos-vs.-random test. The result of one "branch" of the test is a real number $D \in [0, 2]$; close to zero for the deterministic and smooth datasets, and approaching two for the random or discrete datasets. Another "branch" of the test, based on the same mathematical relation, produces two functions that appear to be convergent for deterministic and smooth datasets, but run totally divergent for random or discrete ones. The D-values yielded by deterministic time series, recorded in the periodic and quasiperiodic sorptions of H_2 or D_2 in Pd, are around 0.001. On the other hand, the databases that were presumably random or non-smooth yielded the test results from $D = 0.2$ to $D = 1.9$. Against these benchmarks, the experimental, aperiodic oscillations scored around 0.003 in D, which is much closer to the deterministic than to a random manner.

Keywords Palladium · Hydrogen · Deuterium · Thermokinetic oscillations · Chaos · Microcalorimetry

1 Introduction

Oscillatory heat evolution accompanying the sorption of hydrogen or deuterium in metallic palladium has recently been described in two reports [1,2]. The thermokinetic oscillations can been induced by admixing hydrogen or deuterium with ca. 10 % vol.

E. Lalik (✉)
Jerzy Haber Institute of Catalysis and Surface Chemistry, Polish Academy of Sciences,
ul. Niezapominajek, 30-239 Kraków, Poland
e-mail: nclalik@cyf-kr.edu.pl

of an inert gas, such as He, Ne, Ar, Kr or N_2, prior to its contact with palladium. The frequencies turned out to be functionally dependent on the atomic parameters (the first ionization potential and the square root of atomic mass) of the inert gases being used in the reaction [2]. Apart from specifying conditions for the oscillatory kinetics to occur, the calorimetric experiments have also demonstrated a consistent invariance of the value of the heat of sorption of $H_2(D_2)$ in Pd, which remains the same over a whole range of frequencies observed, independent of whether the oscillations are periodic or quasiperiodic, and irrespective of the process duration. Here, we report occurrence of aperiodic dynamics in oscillatory heat evolution in the H(D)/Pd system and we propose a mathematical test to prove that the calorimetric time series in question represent mathematical chaos rather than a random noise.

Several mathematical methods have been proposed to be used as chaos-vs.-random test. In the effort to detect the symptoms of chaotic behavior in a given dataset (orbit), these methods differ by applying their algorithms either directly to the time series, or to the representations in the phase space. Falling into the first category is the Lyapunov exponent λ that measures an extent of the so-called sensitive dependence on initial conditions (also known as the butterfly effect) which is a defining characteristic of the mathematical chaos [3,4]. The method of surrogate data creates a set of supplementary datasets by rearranging the original time series in such a way as to retain its linear statistical characteristics (like the mean and variance) in order to be able to compare certain statistics, like the correlation dimension [5], computed for the original data, to those computed for the surrogate datasets. Basing on the results of such comparison, there can be rejected or accepted a null hypothesis of the original data as being generated by a linear Gaussian (stochastic) process [6]. Among the phase space using methods, the correlation exponent ν measures the spatial correlation of random points on the trajectory [5]. The method of information dimension σ begins with a partition of phase space into cells of arbitrary dimension l and then applies the Shannon entropy formula to account for the probability of a point to fall within the given cell [7]. In general, therefore, these seemingly most often applied methods make use of certain intrinsic properties of chaos itself rather than of the fundamental fact that chaos is related to a mathematical function whereas randomness, by definition, is not.

In this article, a mathematical relationship is being outlined and proposed to be used as a simple mathematical test that addresses this fundamental difference between chaos and randomness and in doing so makes it possible to distinguish between random or functional character of both the experimental and the computed time series. The validity of the proposed test has been checked against the computed time series, both random and chaotic, as well as against a considerable body of the experimental data that has been obtained from a newly found oscillatory reaction of the sorption of hydrogen in metallic palladium which shows all kinds of nonlinear dynamics including the periodic, quasiperiodic and aperiodic oscillations.

2 Outline of the concept

Consider a function $f(x)$ which is smooth, continuous and square integrable on the interval $[a, b] \subset \mathbb{R}$ (cf. Scheme 1A). Let $f'(x)$ be the first derivative of $f(x)$ (cf.

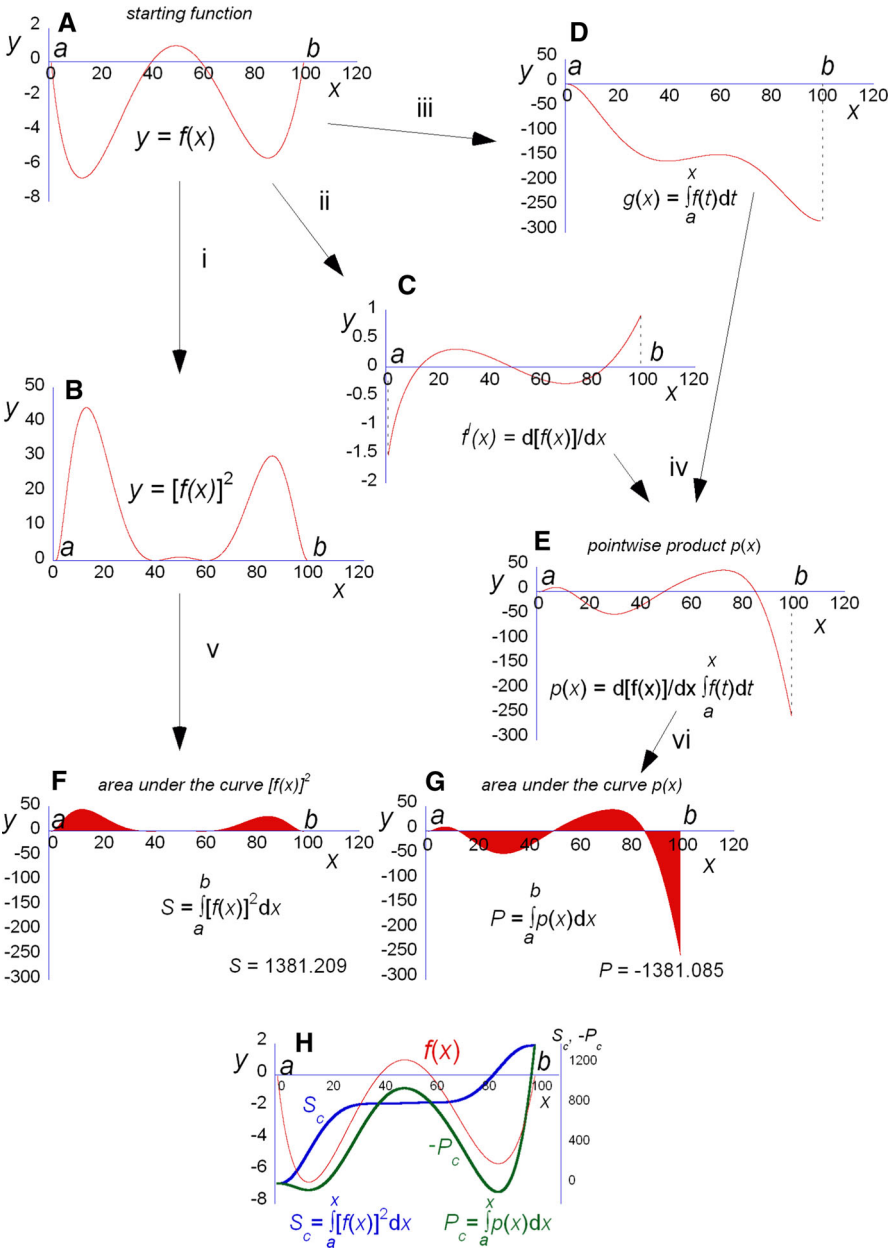

Scheme 1 The essence of relation (4). Starting from a polynomial $f(x)$ (panel **A**), a sequence of mathematical operations (from **i** to **vi**) eventually leads to comparison of a pair of definite integrals, that of the square $[f(x)]^2$ (panel **F**) and that of the pointwise product $p(x)$ (panel **G**), respectively denoted P and S. Both the areas under the curves, highlighted in red, are represented to the same scale in panels **F** and **G**, to facilitate visual comparison. On numerical integration, these red areas turn out to be equal in absolute values but opposite in sign, in agreement with relation (4), even thought it is not immediately evident on visual examination. The polynomial used here scored $D = 0.0000879$ (D is the absolute relative difference of S and P; cf. Sect. 4)

Scheme 1C) and $g(x)$ be an indefinite integral of the $f(x)$ with the variable upper limit on the interval $[a, b]$ (cf. Scheme 1D). We define a function $p(x)$ as the pointwise product of the derivative $f'(x)$ and the integral $g(x)$ (cf. Scheme 1E):

$$p(x) = f'(x)g(x) = \frac{d[f(x)]}{dx} \int_a^x f(t)dt \tag{1}$$

and for $x \in [a, b]$ and $f(x) = 0$, the following relation holds:

$$-\int p(x)dx = \int [f(x)]^2 dx \tag{2}$$

To proof this relation, we note that the integral of the pointwise product $p(x)$ within the interval $[a, b]$, as defined by (1), can be integrated by parts

$$\int \left(\frac{d[f(x)]}{dx} \int_a^x f(t)dt \right) dx = f(x)g(x) - \int \left(f(x) \frac{d}{dx} \int_a^x f(t)dt \right) dx \tag{3}$$

We apply the fundamental theorem of calculus (FTC) to the second term in RHS, and notice that the $f(x)g(x)$ term vanishes for $f(x) = 0$ or $g(x) = 0$, with $x \in [a, b]$, leading to the desired relation:

$$-\int \left(\frac{d[f(x)]}{dx} \int_a^x f(t)dt \right) dx = \int [f(x)]^2 dx \tag{4}$$

Two cases can be considered depending on whether the integration of Eq. (3) is definite or indefinite (with variable upper limit). For the case of the definite integration on the interval $[a, b]$, the Eq. (3) takes the form:

$$\int_a^b \left(\frac{d[f(x)]}{dx} \int_a^x f(t)dt \right) dx = [f(x)g(x)]_a^b - \int_a^b \left(f(x) \frac{d}{dx} \int_a^x f(t)dt \right) dx, \tag{5}$$

which for $f(a) = f(b) = 0$, by virtue of FTC, and on changing the signs to both sides, reduces to

$$-\int_a^b \left(\frac{d[f(x)]}{dx} \int_a^x f(t)dt \right) dx = \int_a^b [f(x)]^2 dx \tag{6}$$

For this case therefore, it follows from relation (4), that if the a and b are both zero crossings of the original function $f(x)$, i.e., for $f(a) = f(b) = 0$, than the areas under the curves of $[f(x)]^2$ and $p(x)$, within the interval $[a, b]$, are equal to each

other in absolute value but opposite in sign. Both sides of (6) represent a real number. For brevity, subsequently the letters P and S will be used to denote, respectively, the integrals in LHS and RHS of (6). Since S is always positive, then P must be negative, and so $S = |P|$ for the conditions under which the Eq. (6) holds. This is illustrated in Scheme 1: both the areas S and P are represented in red in Scheme 1F and G, respectively. It should be noticed, that Eq. (6) is also true for $f(a) = 0$, $f(b) \neq 0$ and $g(b) = 0$, as the $f(x)g(x)$ term in Eq. (5) vanishes at these conditions as well, but this is of less relevance to a potential test application of formula (6).

The second case involves indefinite integration with variable upper limit of (3), whence by virtue of relation (4) we obtain the following:

$$-\int_a^x \left(\frac{d[f(x)]}{dx} \int_a^x f(t)dt \right) dx = \int_a^x [f(x)]^2 dx \tag{7}$$

The integrals in RHS and LHS of (7) represent two functions, denoted S_C and P_C, respectively. The plots representing the integral S_C and the negative of integral P_C (denoted $-P_C$) intersect for $f(x) = 0$, or $g(x) = 0$. This is illustrated in Scheme 1H. The two lines representing S_C (blue) and $-P_C$ (green) are both plotted against the right-hand side axis. It can be seen, that all intersection points of the two lines coincide with zero points of the original function $f(x)$ (in red, plotted against the left-hand side axis). There are also possible cases of S_C and $-P_C$ intersecting for $g(x) = 0$ and $f(x) \neq 0$, not represented in this example.

3 Experimental

The experimental procedure leading to periodic or quasiperiodic oscillatory sorption of $H_2(D_2)$ in Pd has been recently described in detail in Ref. [1,2]. The oscillatory kinetics begins with a fresh Pd powder and, after a 20- 30 min, the oscillations cease (in most cases) when the Pd sample is saturated (cf. Fig. 1A, C), i.e., a state of dynamic equilibrium between the hydride and the $H_2(D_2)$ in the gas phase is being reached. However, aperiodic time series were obtained from Pd sample being already saturated with hydrogen, with the D_2/Kr or H_2/N_2 mixture still flowing through the sample bed. It has been found possible to induce oscillatory heat evolution in this stage by connecting the system to a water aspirator with somehow irregular suction. The aperiodic response so induced differs from either the periodic or the quasiperiodic kinetics in that the aperiodic time series oscillates around the zero line (cf. Figs. 1E, 2).

Figure 2 shows the sorption of a D_2/Kr mixture in a 0.23 g sample of fine-grained Pd powder (granularity less then 75 μm, supplied by Aldrich). Starting with a fresh metal, the reaction is first accompanied by exothermic oscillations, with the power spectrum (cf. the lower left inset) indicative of quasiperiodic dynamics with two frequencies of 0.0240 and 0.0613 Hz. The integration of the calorimetric curve for this quasiperiodic stage, i.e., from a start to around 4,000 s, yields the total heat evolution of ca. 17,000 mJ (ca. 0.07 kJ/g Pd). This thermal effect turns out to be slightly below the average amount

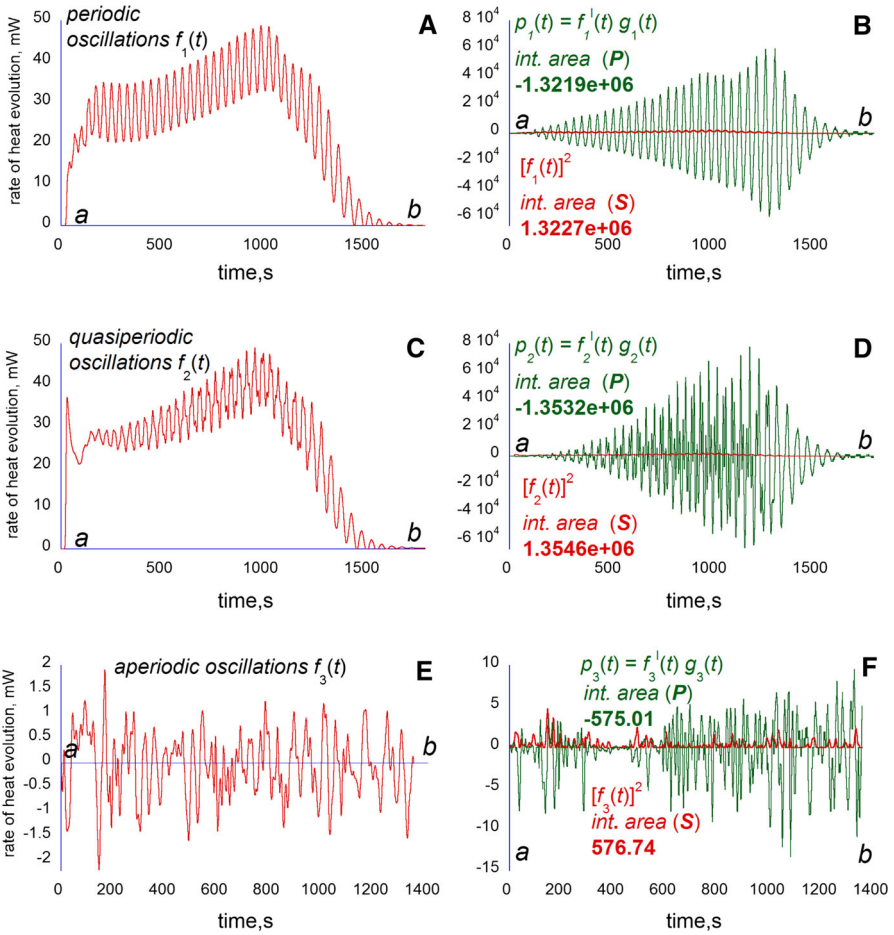

Fig. 1 Using formula (6) to detect determinism in experimental datasets recorded with gas flow-through microcalorimeter on the oscillatory sorption of hydrogen (or deuterium) in metallic palladium. The left-hand panels **A**, **C** and **D** show the original calorimetric time series $f_n(t)$, while the right-hand ones compare their corresponding pointwise product curves $p_n(t)$ (*green*) and their squares $[f_n(x)]^2$ (*red*). The areas under the *green* (P) and *red* (S) curves are equal in absolute values but opposite in signs (within an error), in agreement with relation (4), indicative of deterministic origin of the examined time series (Color figure online)

of heat recorded on reaching saturation for this Pd sample (ca. 0.09 kJ/g Pd) under the same conditions [2]. Hence, at the point of 4,000 s the Pd sample must be rather close to the state of saturation with deuterium. The dynamics of oscillations clearly changes at ca. 4,000 s and the corresponding power spectrum (cf. the upper right inset) confirms the aperiodic dynamics of oscillations after this point. During this aperiodic stage, the calorimetric curve, representing the rate of heat evolution, oscillates from above to below zero, but on integration, a net heat evolution turns out to be only −440 mJ, an effect negligible within experimental error. It indicates that both the exothermic and the endothermic effects are on average equal (within en error) in the long run. It

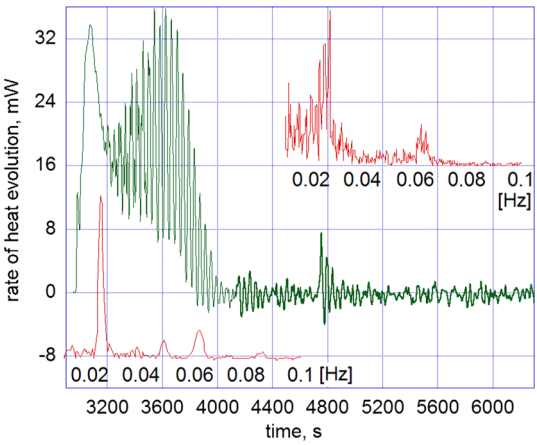

Fig. 2 Thermokinetic oscillations in the sorption of D_2 (admixed with ca. 10 % of Kr) in palladium powder at the temperature of 75 °C. The sustained aperiodic oscillations develop on Pd saturated with deuterium (at ca. 4,000 s), following a stage of the periodic oscillations accompanying the sorption process proceeding far from a dynamic equilibrium. *Insets* show the power spectra (*red*), separately for the periodic (*lower left*) and the aperiodic oscillations (*upper right*) (Color figure online)

appears that the aperiodic thermokinetic oscillations may accompany a non-periodic sorption-desorption process, which apparently can proceed indefinitely, and with an overall zero heat production in the long term. It should be stressed, that a necessary condition for such oscillations to occur is that the reaction mixture must continue to flow through the Pd powder sample, while the system is being subjected to the irregular pressure changes.

There are several advantages of using the time series recorded in the thermokinetic oscillations of sorption of $H_2(D_2)$ in Pd as the probe datasets for formulae (6) and (7). First, it is natural for the calorimetric curves to start and end at zero, so the condition of $f(a) = f(b) = 0$ (necessary for (6) to be used; cf. previous section) is readily met. Second, the calorimetric curves obtained in the experiments are practically noiseless, in other words they are smooth. Thirdly, the microcalorimetric time series are continuous, since they represent a constant process of heat evolution. Finally, the process can exhibit all kinds of different oscillatory dynamics and the microcalorimetric experiments show very high reproducibility [1,2].

4 Application of the test procedure

Two "branches" of the test, respectively applying formula (6) and formula (7) to the examined datasets can be devised.

4.1 Using formula (6)

The Eq. (6) is true for a continuous, smooth and square integrable function $f(x)$, so the reals S and P should be equal for such datasets, but not so for a random sequence. A departure from Eq. (6) should therefore indicate discontinuity and possibly randomness. Any dataset can be use as a staring function $f(x)$ and have its values of S and P computed numerically. For the polynomial used as the illustration in Scheme 1, we obtain $S = 1{,}381.209$ and $P = -1{,}381.085$, which may be considered equal

within a numerical error. For the real-life data, the S and P may also be affected by an experimental error, so usually the two reals will not be strictly equal. A parameter to evaluate how close to equal the S and P are is therefore needed, and also we want such parameter to be invariant to the size of the datasets under examination. To this end, we define the absolute relative difference (ARD) of S and P according to the following formula:

$$D = \left| \frac{S - |P|}{0.5(S + |P|)} \right| = 2 \left| \frac{R - 1}{R + 1} \right|, \tag{8}$$

where $R = S/|P|$, and note that $D \to 0$ as $R \to 1$, and $D \to 2$ as $R \to \infty$, or $R \to 0$. Consequently the test yields a real number $D \in [0, 2]$, independent of the dataset sizes. As a benchmark, it will be close to zero for continuous and smooth, and hence deterministic datasets, i.e., for $S \approx -P$. Conversely, the more disparate the values of S and $-P$, the closer D values will be approaching two. The latter will be indicative of discontinuous and non-smooth data, and possibly of a random character of the examined datasets. For the polynomial used as a "handle" in Scheme 1 we obtain $D = 0.0000879$.

Figure 1 shows examples of application of the test to real-life datasets, namely, to a periodic f_1, quasiperiodic f_2 and aperiodic f_3 time series recorded on experiments with thermokinetic oscillations in the sorption of hydrogen (f_1 and f_2; Fig. 1A–D) or deuterium (f_3; Fig. 1E, F) in palladium powder. The figures on the left show the original calorimetric time series. Each dataset has been subjected to the test procedure, i.e. a sequence of operations as illustrated in Scheme 1. In Fig. 1B, D, and F, the corresponding pointwise products are plotted in green, and the squares $[f_1]^2$, $[f_2]^2$ and $[f_3]^2$ are plotted in red, to the same scale. The respective values of areas under both the square curves and the pointwise product curves, denoted, respectively S and P, have also been shown in Fig. 1B, D and F. The values of D for f_1, f_2 and f_3, turned out to be, respectively $D(f_1) = 0.00060501$, $D(f_2) = 0.0010340$ and $D(f_3) = 0.0030041$. Both the periodic and quasiperiodic datasets f_1 and f_2 are certainly deterministic. The aperiodic dataset f_3 (Fig. 1E, F) appears to score highest in D, but still much closer to zero than to the upper limit of 2, which points out to the deterministic rather than random character of f_3.

4.2 Using formula (7)

Instead of comparing the reals S and P resulting from (6), it is possible to compare the plots representing integrals with variable upper limits defined in formula (7). Figure 3 shows the behavior of the curves S_C and $-P_C$ for two real-life datasets f_1 and f_3 (the same as shown in Fig. 1A, E, respectively), in addition to a random sequence, namely a string of 3,000 digits of π number [8] denoted f_4. The dataset f_1, represents the periodic thermokinetic oscillations, and is shown in red in Fig. 3A, B. The blue curve represents the indefinite integral with variable upper limit of the squared f_1 (RHS of (7)), whereas the green curve represents the indefinite integral of the pointwise product defined in LHS of (7), both plotted against the right-hand side axis in Fig. 3A, B. The real-life oscillations proceed far from equilibrium (in thermodynamic sense), meaning that for most of the duration of the experiment, the red curve is staying well above the

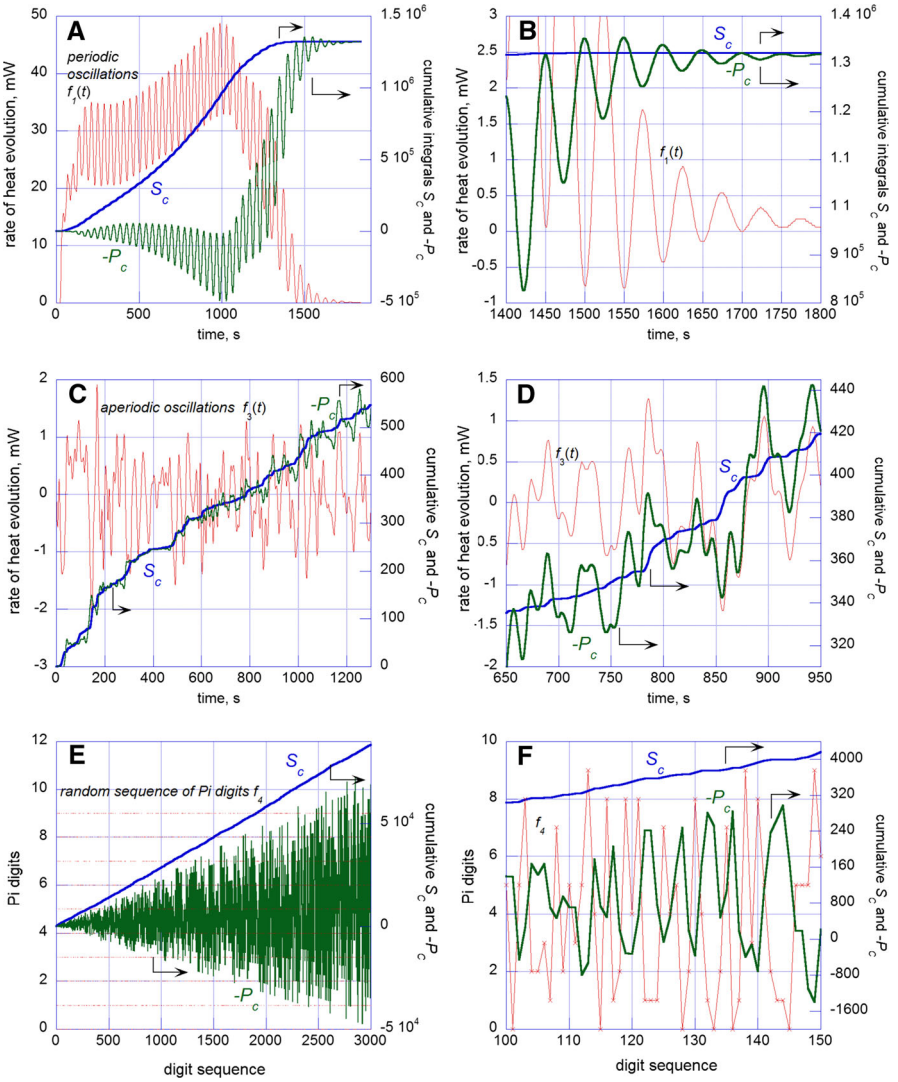

Fig. 3 Using formula (7) to detect determinism in the experimental time series **A**–**D** in comparison to a random sequence of π digits (**E**, **F**). Determinism of the datasets $f_1(t)$ and $f_3(t)$ is indicated by intersections of the S_C (*blue*) and P_C (*green*) curves coinciding with the zero points of the original curves (*red*). To appreciate this effect certain fragments are enlarged in the right-hand panels **B** and **D**. On the other hand, the divergent behavior of S_C and P_C curves characteristic for random datasets can be seen in panels **E** and **F** (Color figure online)

zero line. However, when the process is nearing to completion (due to saturation of Pd sample with hydrogen) the red curve does make a few dumped oscillations, actually crossing the zero line several times (cf. Fig. 3B), before reaching final equilibrium. The periodic reaction kinetics is certainly deterministic and hence, in agreement with relation (4), the few zero points in the red curve coincide with intersections of the blue

and green curves, as can be seen more clearly in Fig. 3B, showing enlarged the period close to the end of the sorption process.

The experimental dataset f_3 (Fig. 3C, D) represents the aperiodic oscillations accompanying the reaction of deuterium with palladium (also shown in Fig. 1E). In this case, the calorimetric time series (red) oscillates around the zero line, which seems to suggest that the deuterium/palladium system is in dynamic equilibrium (in thermodynamic sense). Here the zero points are numerous. Note however, that for each zero in the red, there corresponds an intersection of the blue and green curves (cf. Fig. 3D for enlargement), thus showing agreement with relation (4). Visually the green curve looks as though it was oscillating around the blue one. In fact, it can be proposed that the S_C and $-P_C$ both converge uniformly to a common limit function. Such convergent behavior is consistent with the relation (4), evidencing a deterministic, and hence mathematically chaotic character of the aperiodic, thermokinetic oscillations represented by this dataset. The same convergent behavior of the S_C and $-P_C$ curves has also been observed when similar aperiodic oscillations were recorded with hydrogen rather than deuterium being sorbed in palladium under the same reaction conditions (not shown).

Figures 3E, F show strikingly different behavior of the S_C and $-P_C$ curves obtained for a random numbers represented by dataset f_4. The sequence of 3,000 digits of π is neither continuous nor a smooth function, and so it does not match the assumptions under which the relation (4) holds. In fact, Fig. 3E shows that the curves S_C and $-P_C$ never cross each other, except that they both start from zero. The same totally divergent behavior of the S_C and $-P_C$ curves has been confirmed for a larger sequence of 250,000 digits of π (not shown).

It should be noted, that both the f_3 and f_4 datasets are visually aperiodic, but it is difficult to tell the deterministic f_3 from the random f_4 solely on visual inspection of the respective plots (compare the red traces in Fig. 3D, F). However, the contrasting behavior of their corresponding S_C and $-P_C$ curves reveals the difference very clearly. Likewise, the value of D calculated using formula (6) for the aperiodic datasets f_3 and f_4, turned out to be $D(f_3) = 0.0030041$ and $D(f_4) = 0.24783$, therefore in spite of both databases being visually aperiodic, the much lower score in D by f_3 points out, again, to its deterministic origin.

A similar point is illustrated in Fig. 4. The figure compares the behavior of S_C and $-P_C$ curves obtained for three types of computed time series, all three visibly aperiodic. However, only one of them, namely the Lorenz chaotic time series $f_5(t)$ is deterministic as well as continuous and smooth, while the Hennon chaotic map $f_6(t)$ is deterministic but non-continuous; and the random Fibonacci sequence $f_7(n)$, is non-deterministic and non-continuous [9]. It can be seen, that only the Lorenz system behaves in accordance with the relation (4) (Fig. 4A, B), as intersections of the S_C and P_C curves coincide with the zero-points of original time series (cf. Fig. 4B for enlargement). On the other hand, the Hennon map yields the curves S_C and P_C clearly divergent, similar to those obtained for the sequence of π digits shown Fig. 3C, D. Here the test fails to detect determinism in the Hennon mapping. This is because in spite of the map being deterministic it is nevertheless not smooth and not continuous, and as such does not match the assumptions under which the relation (4) holds. Finally, for the random Fibonacci sequence (Fig. 4E, F), the test procedures send the S_C and P_C

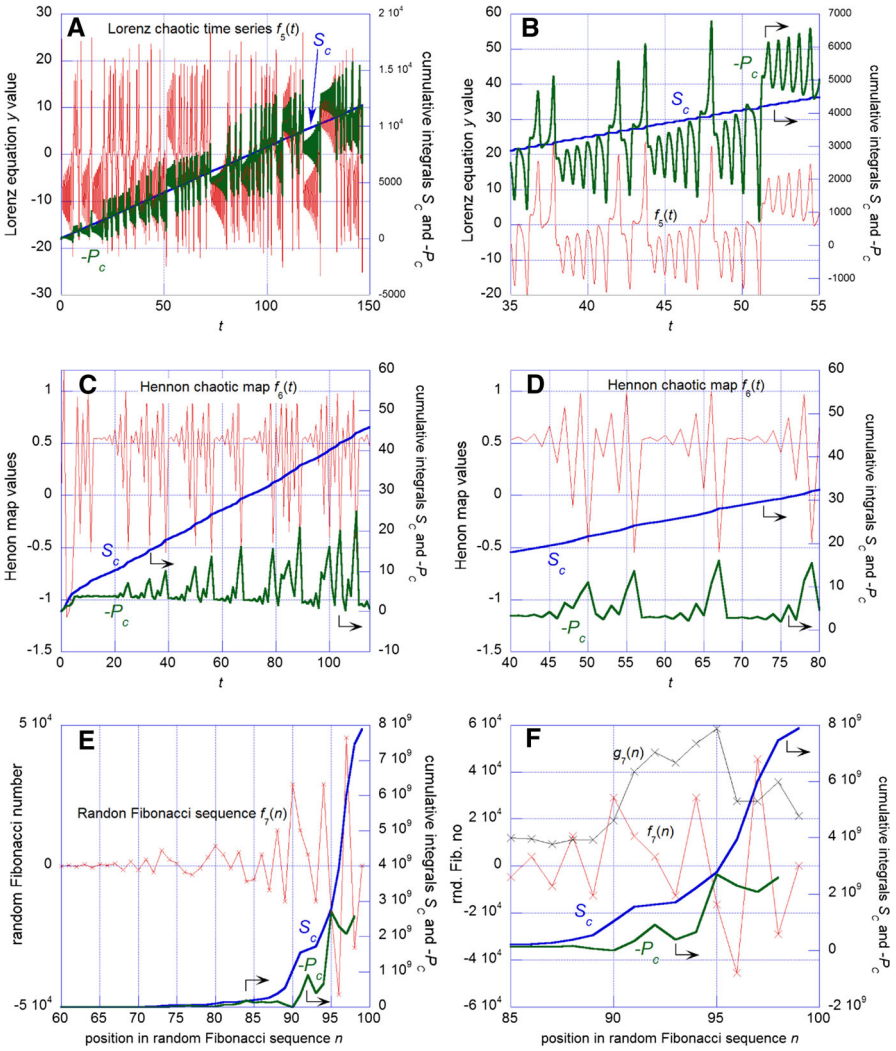

Fig. 4 Using formula (7) to detect determinism in a three computed time series: **A** deterministic and continuous a chaotic Lorenz curve; **C** deterministic but not continuous a Hannon chaotic map; **E** not deterministic and not continuous a random Fibonacci sequence. The S_C (*blue*) and P_C (*green*) curves confirm determinism for the Lorenz chaos, showing intersections coinciding with zero points of the original Lorenz time series (cf. the blown up fragment in panel **B**). However, the S_C and P_C curves run totally divergently for the Hennon map (cf. panels **C**, **D**), in spite of its obvious determinism, no doubts because of its being discrete rather than continuous, and the same divergent behavior of the curves S_C and P_C can be observed for the random Fibonacci sequence (cf. panel **E** and the enlargement in **F**) (Color figure online)

curves definitely diverging, and although the green P_C curve does incidentally near the blue one (S_C) at $n = 95$, yet this does not coincides with any zero point neither in the original dataset (red), nor in the plot of its indefinite integral $g_7(n)$ (shown in black in Fig. 4F).

Table 1 The D-scores, calculated with formula (8), for the datasets tested and the reals S and $-P$ calculated with formula (6)

Dataset examined	S	$-P$	D
Polynomial in Scheme 1 (cmptd.)	1,381.209	1,381.085	0.0000879
Periodic oscillations (exp.), f_1	1.3227e+06	1.3219e+06	0.00060501
Quasiperiodic oscillations (exp.), f_2	1.3546e+06	1.3532e+06	0.0010340
Aperiodic oscillations (exp.), f_3	576.74	575.01	0.0030041
A sequence of 3,000 digits of π (cmptd.), f_4	88,414	68,918	0.24783
Lorenz chaos (cmptd.), f_5	11,873	11,802	0.0060459
Hennon chaotic map (cmptd.), f_6	56.979	1.1718	1.9194
Random Fibonacci sequence (cmptd.), f_7	7.8840e+09	2.5798e+09	1.0138

exp. experimental, *cmptd.* computed

As for testing with formula (6), using (6) and (8) to calculate D values for the datasets presented in Fig. 4, we obtain $D(f_5) = 0.0060459$ ($S = 11873$; $P = -11802$) for the Lorenz chaos, $D(f_6) = 1.9194$($S = 56.979$; $P = -1.1718$) for the chaotic Hennon map, and $D(f_7) = 1.0138$($S = 7.8840e+09$; $P = -2.5798e+09$) for the random Fibonacci sequence (cf. Table 1).

5 Discussion

The test seems to be relatively simple and quick. It can be applied to real life datasets directly (rather than to a phase space representation), using the formulae (6) or (7), and it does not require any surrogate datasets to be created. In the case of using formula (6) the test conveniently yields a real number $D \in [0, 2]$ as the score, so that the result can be immediately assessed. The only requirement for the dataset itself is that it has to start and end at zero for applying formula (6) to it, but it is not needed for using formula (7). On the other hand, a meaningful use of the test requires certain prior knowledge of the source of the datasets tested, particularly in using formula (6). Table 1 summarizes the D-scores obtained for the datasets subjected to the test procedure and presented in Figs. 1, 3 and 4. The result for the polynomial used in Scheme 1 is understandably the closest to zero (0.0000879). The periodic oscillations f_1 scored the second best (0.00060501), and the quasiperiodic oscillations f_2 came only marginally higher (0.001034). The gas flow-through microcalorimetric technique used to obtain the oscillatory curves f_1 and f_2 (as well as f_3) makes it possible to record practically noiseless data. No doubts because of this high signal to noise ratio, the experimental error did not weight significantly on the test results in those cases. In fact, the experimental datasets f_1 and f_2 scored approximately only by one order of magnitude higher than the computed polynomial. This level of D turned out to be typical, and has been confirmed for a considerable body of over hundred oscillatory sorption/desorption cycles in the $H_2(D_2)$/Pd system that have been carried out to date in our laboratory [1,2].

It is a major purpose of this work to detect determinism in the aperiodic oscillations f_3 recorded in the sorption of D_2 in Pd. The D for this system (0.0030041) turned out to be very similar to that obtained for quasiperiodic oscillations f_2. At the same time, another deterministic dataset, the Lorenz chaotic curve f_5, scored even slightly higher than f_3, in spite of f_5 being computed rather than experimental. Hence, the D-score for f_3 comes out well within the range of D expected for deterministic datasets. Using formula (7) confirms the deterministic character of aperiodic oscillations represented in dataset f_3 (cf. Fig. 3C, D). The characteristically convergent behavior of its S_C and P_C curves is analogous to that manifested by S_C and P_C curves obtained from the datasets f_1 and f_5. For all three datasets, the intersections of S_C and P_C coincide with zero points in the original datasets, in accordance with relation (4), indicative of the data being smooth and continuous, and hence being of deterministic origin. Since it is aperiodic and deterministic at the same time, therefore, the dataset f_3 must represent mathematical chaos. Thus, the thermokinetic oscillations f_3 appears to be a manifestation of chaos in oscillatory heat evolution accompanying the reaction of hydrogen (deuterium) with palladium. To our best knowledge, it is the first time that the chaotic dynamics in this system is being reported.

For the discontinuous, discrete datasets f_4, f_6 and f_7, their S_C and P_C curves have no intersections, apart from initial points, and are apparently divergent. Thus, application of formula (7) cannot detect determinism in the Hannon map f_6. Likewise, the D scores of the discontinuous and/or random datasets are the highest, in fact, the Hennon map yielded D as high as 1.9194, which is very close to the upper limit of two. Again therefore, the formula (6) expectedly failed to detect determinism in the Hennon maps, as it is neither a continuous nor a smooth function. The formulae (6) and (7) provide therefore more a test for smoothness rather than determinism, however, it can be argued, that smoothness itself implies determinism [10,11]. On the other hand, in cases when a deterministic, but a discrete map may actually be expected from the experiments, an occasional low score in D may possibly indicate that somehow deterministic in nature, but unexpected by researchers a by-process, or a perturbation, may be taking place in the experimental system.

6 Conclusions

Aperiodic, thermokinetic oscillations have been recorded calorimetrically in the reaction of sorption of hydrogen in palladium. An expression relating the integral of a square of a function $f(x)$ with the integral of a pointwise product of the first derivative of $f(x)$ and the indefinite integral with variable upper limit of $f(x)$ has been formulated and proved. Basing on this relation, two procedures to distinguish random from determinism has been proposed. The results of such tests applied to aperiodic, calorimetric time series suggest, that the aperiodic oscillations demonstrate the chaotic dynamics in the reaction of hydrogen or deuterium with the metallic palladium. At the same time, the results demonstrate diagnostic value of the newly proposed test.

Acknowledgments The author is grateful to the late Dr A. J. Groszek and to Microscal Ltd., London, for support and assistance.

7 Appendix: Differential and difference equations used to obtain the computed time series

The Lorenz equations were integrated numerically using the fourth order Runge-Kutta method for the same set of initial conditions: t = 0; $x_0 = 5$; $y_0 = 0$; $z_0 = 5$, and a step h = .003 s. A QuickBasic program for Runge-Kutta integration has been taken from Ref. [12]. The program was slightly modified by the present author to enable writing of integration results into a datafile. The chaotic dynamics has been confirmed using the power spectra and phase portraits (not shown). The Lorenz equations in the form:

$$\begin{aligned} \frac{dx}{dt} &= 10(y - x), \\ \frac{dy}{dt} &= x(r - z) - y, \\ \frac{dz}{dt} &= xy - \frac{8}{3}z \end{aligned} \tag{9}$$

was integrated for r=28.

The Hennon equation was iterated using a simple QuickBasic program written for this purpose by the author. The equations:

$$\begin{aligned} x_{n+1} &= 1 - ax_n^2 + y_n, \\ y_{n+1} &= by_n \end{aligned} \tag{10}$$

was iterated for $a = 1.55$ and $b = 0.3$ starting with $x_0 = 0.02$ and $y_0 = 0.2$.

References

1. E. Lalik, J. Haber, A.J. Groszek, J. Phys. Chem. C **112**, 18483 (2008)
2. E. Lalik, Chem. Phys. **135**, 064702 (2011)
3. A. Wolf, J.B. Swift, H.L. Swinney, J.A. Vastano, Physica D **16**, 285 (1985)
4. Ch. Skokos, Lect. Notes Phys. **790**, 63 (2010)
5. P. Grassberger, I. Procaccia, Physica D **9**, 189 (1983)
6. T. Schreiber, A. Schmitz, Physica D **142**, 346 (2000)
7. D.J. Farmer, Z. Naturforsch, A **37**, 1304 (1982)
8. H.J. Smith, *PiW—Compute Pi to a Million or so Decimal Places in Windows*, Version 1.31, 1994, Copyright (c) 1981–1994 by author: Harry J. Smith, 19628 Via Monte Dr., Saratoga, CA 95070. All rights reserved. http://harry-j-smith-memorial.com/Pi/PiW.html
9. D. Visvanath, Math. Comput. **69**, 1131 (1998)
10. L.W. Salvino, R. Cawley, Phys. Rev. Lett. **73**, 1091 (1994)
11. G.J. Ortega, E. Louis, Phys. Rev. Lett. **81**, 4345 (1998)
12. D. Acheson, *From Calculus to Chaos* (Oxford University Press, Oxford, 1997)